

# Performance of a Cellulose Acetate Permeator with Permeability-Influenced Feed

K. Li  
D. R. Acharya  
R. Hughes

Department of Chemical & Gas Engineering  
University of Salford  
Salford M5 4WT, England

The dependence of permeabilities on the operating conditions, such as the pressure and the feed composition, is well recognized, particularly when an asymmetric cellulose acetate type of membrane is employed (Donahue et al., 1989; Rangarajan et al., 1984). This behavior suggests that if constant values of the permeabilities are assumed in the design calculation, a serious error may occur resulting in either under- or overdesign of the separation system. While considerable design work has been carried out in the past using cellulose acetate membranes (for example, Pan, 1983; Perrin and Stern, 1986; Sidhoum et al., 1988), a constant value of permeability has been used in all these studies, which may not be the case for certain gases and when large pressure differences exist across the membrane (Donahue et al., 1989; Rangarajan et al., 1984).

Chern et al. (1985), in a study of hollow-fiber permeator design, used a dual-sorption model which predicted a permeability decrease as the feed pressure is increased. As pointed out by Lee et al. (1988), however, in situations where the permeability increases with increase in feed pressure, the presence of a less permeable component reduces the permeability of the more permeable gas while the presence of a more permeable component increases the permeability of a less permeable gas; this behavior is not adequately described by the dual-sorption model.

The objective of this study was to investigate the effect of variable permeabilities on the performance of a permeator employing a cellulose acetate type of membrane. The experiments were conducted using a CO<sub>2</sub>-N<sub>2</sub> mixture. The variation in the permeabilities of CO<sub>2</sub> and N<sub>2</sub> with the pressure and the feed composition has been measured experimentally, and statistical models have been fitted to the data. The experimental data, i.e., the stage cut and the resultant CO<sub>2</sub> concentration in the unpermeated stream, have been compared with theoretical results obtained using a perfect mixing model which incorporated variable permeabilities.

## Experimental Study

The membrane permeator designed for the present experiments was essentially a high-pressure vessel containing the cellulose acetate membrane in thin sheet form. The membrane (asymmetric type, manufactured by W.R. Grace Co.) was supported by a bronze sinter (average pore size 60  $\mu$ m, 62 mm dia., 3 mm thick) which separated the permeator into two compartments. The feed was introduced into one of the compartments at a desired flow rate and at a constant total pressure  $p_u$ . The feed permeates into the second compartment which is also maintained at a constant pressure,  $p_p$  ( $< p_u$ ). The feed is thus partitioned into two product streams, i.e., a permeated low-pressure stream and an unpermeated high-pressure stream. The pressure on the permeate side was atmospheric in all cases, while the pressure on the feed side was varied up to 2,300 kPa. The membrane area was constant for all experiments; however, the stage cut was varied from about 0.1 to 0.47 and the corresponding feed flow rate range was 0.014 to 0.002 m<sup>3</sup>/h. The feed rate and unpermeate flow rate was controlled by mass flow controllers, and CO<sub>2</sub> concentrations in both permeate and unpermeate side were measured using a standard infrared analyzer.

## Results

### Permeability measurements

The ability of a gas to permeate through a polymeric membrane is a phenomenon usually expressed as a permeability defined by:

$$P = \frac{J\delta}{\Delta p} \quad (1)$$

where  $J$  is the steady-state flux of the permeate gas,  $\Delta p$  is the pressure difference across the membrane, and  $\delta$  is the membrane thickness. The permeability in Eq. 1 represents a measure of permeation through not only the membrane but also the

Correspondence concerning this paper should be addressed to R. Hughes.

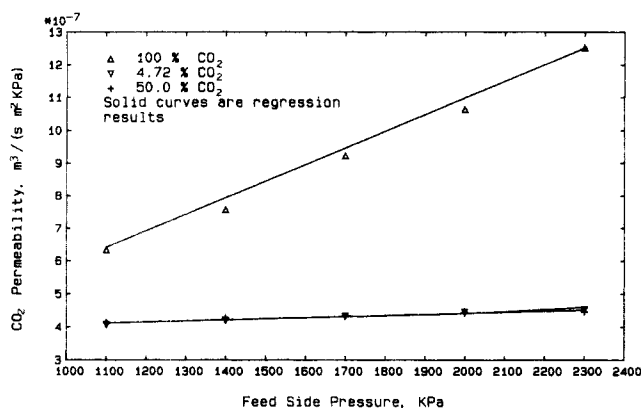


Figure 1. CO<sub>2</sub> permeability in CO<sub>2</sub>/N<sub>2</sub> mixtures.

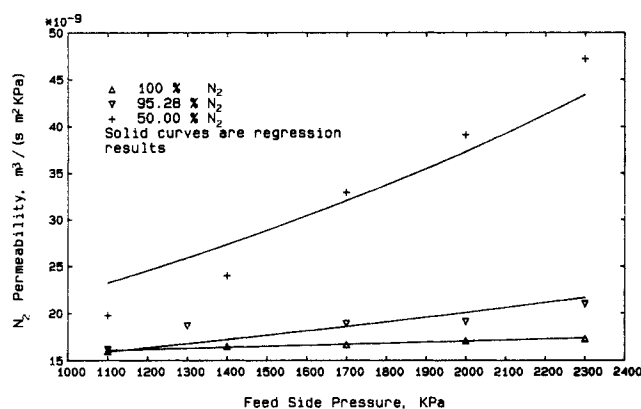


Figure 2. N<sub>2</sub> permeability in CO<sub>2</sub>/N<sub>2</sub> mixtures.

boundary layers on both sides of the membrane because bulk pressures are used. Therefore, any physical effects on the boundary layer regions are included in the permeability so defined. In this study, experimental measurements on the specific permeabilities of CO<sub>2</sub> and N<sub>2</sub> (defined as  $P/\delta$ ) were made for a given membrane while the flux of the permeating gas was measured for different values of  $\Delta p$ . The pressure ratio across the membrane was varied from 11 to 23 and two feed compositions: 4.72% CO<sub>2</sub> in N<sub>2</sub> and 50% CO<sub>2</sub> in N<sub>2</sub> were considered. The flow rate of the feed mixture was maintained at significantly higher levels than the permeate flow rate so that the membrane performance could be evaluated at a constant gas composition. Experiments were also conducted on pure CO<sub>2</sub> and N<sub>2</sub> to obtain the effect of the presence of N<sub>2</sub> on CO<sub>2</sub> permeabilities and *vice versa*. The results obtained from these experiments are discussed below.

Figure 1 shows the variation in measured permeabilities with the feed pressure and the feed composition for CO<sub>2</sub>. It can be seen from the figure that in the case of pure CO<sub>2</sub>, a twofold increase in the feed pressure results in a similar increase in the permeability. In fact, a linear relationship between the feed pressure and the permeability appears to exist in the pressure range studied. It is interesting to note that the magnitude of the CO<sub>2</sub> permeabilities decreases significantly when the feed consisted of CO<sub>2</sub>-N<sub>2</sub> mixtures: by 30% at lower feed pressures and to one third of the pure gas value at higher feed pressures. The figure also shows that in the case of mixtures, the CO<sub>2</sub> permeability is virtually independent of the feed pressure and does not change with the feed composition even when the CO<sub>2</sub> concentration in the feed was changed from 4.72% to 50% CO<sub>2</sub>.

Totally different behavior is obtained for the case of N<sub>2</sub> permeabilities as shown in Figure 2. The pure-component permeability of N<sub>2</sub> remains more or less unchanged with increasing feed pressures. At the same time, the presence of CO<sub>2</sub> in the feed stream actually results in an increase in the N<sub>2</sub> permeability by a factor of nearly 3 at a pressure ratio of 23 and when the feed contains 50% CO<sub>2</sub>. The reason for this behavior is not clear; however, similar results have been obtained by Donahue et al. (1989) for CO<sub>2</sub>/CH<sub>4</sub> mixtures who reported that the CH<sub>4</sub> permeability is increased by the presence of CO<sub>2</sub>.

The data of Figures 1 and 2 have been fitted to statistical expressions of the types:

$$P_i = P_i^o + \sum_{j=1}^n \alpha_{ij} p_i \quad (2)$$

and

$$P_i = P_i^o \exp \left( \sum_{j=1}^n \alpha_{ij} p_i \right) \quad (3)$$

where  $\alpha_{ij}$  and  $P_i^o$  are constants, values of which together with the regression results are summarized in Table 1. The models that gave the higher value of the *R*-square were plotted in the curves shown in Figures 1 and 2 and were also used in the separation analysis which is discussed below.

### Separation Measurements

A perfect mixing model, which was detailed elsewhere (Stern, 1972) and incorporated the statistical models of Eqs. 2 and 3,

Table 1. Models for Permeability Data

Component	Regression Equation	$\alpha_A$	$\alpha_B$	$P_A^o$	$P_B^o$	<i>R</i> -sq %
Pure CO <sub>2</sub>	$P_A = P_A^o + \alpha_A p_A$	$5.09 \times 10^{-10}$		$8.12 \times 10^{-8}$		99.1
	$P_A = P_A^o \cdot \exp(\alpha_A \cdot p_A)$	$6.294 \times 10^{-4}$		$2.998 \times 10^{-7}$		98.9
Pure N <sub>2</sub>	$P_B = P_B^o + \alpha_B \cdot p_B$		$1.095 \times 10^{-12}$		$1.488 \times 10^{-8}$	98.9
	$P_B = P_B^o \cdot \exp(\alpha_B \cdot p_B)$		$6.3 \times 10^{-5}$		$1.508 \times 10^{-8}$	98.6
Binary Mixture of N <sub>2</sub> and CO <sub>2</sub>	$P_A = P_A^o + \alpha_{AA} \cdot p_A + \alpha_{AB} \cdot p_B$	$3.34 \times 10^{-11}$	$3.255 \times 10^{-11}$	$3.76 \times 10^{-7}$		94.3
	$P_B = P_B^o + \alpha_{BA} \cdot p_A + \alpha_{BB} \cdot p_B$	$3.164 \times 10^{-11}$	$7.586 \times 10^{-12}$		$3.687 \times 10^{-9}$	88.1
	$P_A = P_A^o \cdot \exp(\alpha_{AA} p_A + \alpha_{AB} \cdot p_B)$	$8.302 \times 10^{-5}$	$7.525 \times 10^{-5}$	$3.79 \times 10^{-7}$		93.0
	$P_A = P_A^o \cdot \exp(\alpha_{BA} \cdot p_A + \alpha_{BB} \cdot p_B)$	$1.09 \times 10^{-3}$	$2.31 \times 10^{-4}$		$1.186 \times 10^{-8}$	91.5

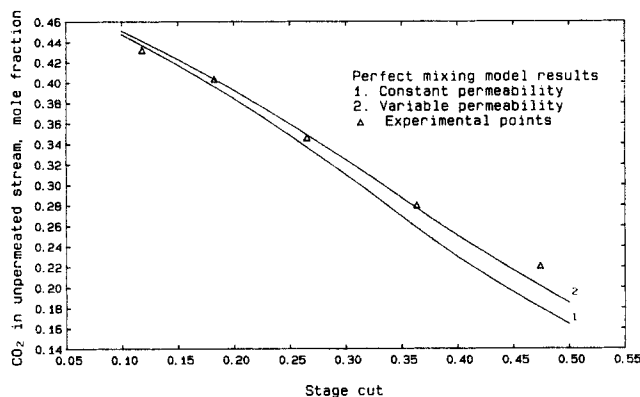


**Figure 3. Stage cut vs. CO<sub>2</sub> concentration in unpermeate stream (pressure ratio across the membrane = 11).**

has been used to predict the performance of a flat sheet permeator. The modeling results have been compared with the experimental results in Figures 3 and 4. As can be seen from Figure 3, where the stage cut is plotted against the CO<sub>2</sub> concentration in the unpermeate stream, the experimental data are in good agreement with the theoretical results when a variable permeability model is used. In addition, if constant

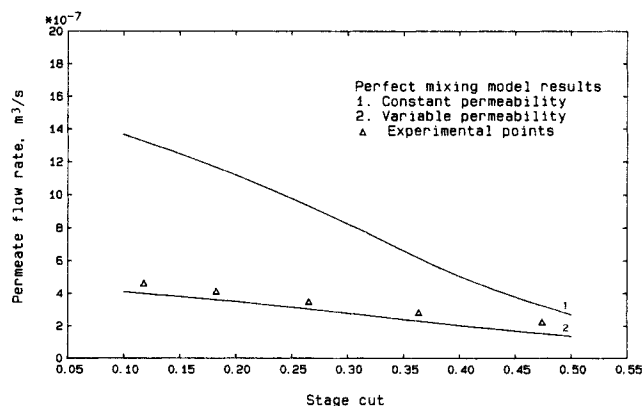


**Figure 4. Stage cut vs. total permeate flow rate (pressure ratio across the membrane = 11).**

permeability is assumed in the model, lower values of CO<sub>2</sub> concentrations in the unpermeate stream are obtained compared to those obtained using variable permeabilities. Admittedly, the difference between the two curves is probably not great. This is because the enrichment or depletion of the feed stream depends on the separation factor (ratio of permeabilities of the two components) which may not significantly change, although the magnitude of the permeabilities may have changed significantly. This change in the magnitude of the permeability should result in a significant change in the permeate flow rate, as shown in Figure 4. It can be seen that the assumption of constant permeability would result in the prediction of significantly higher permeate flow rate, by a factor of 3.5 at a stage cut of 0.1. This would thus result in gross underdesign of the permeator, should the basis of design be the required quantity of the permeate.

### Acknowledgment

Financial assistance from the Procurement Executive MOD and SERC is gratefully acknowledged.

### Literature Cited

- Chern, R. T., W. J. Koros, and P. S. Fedkiw, "Simulation of the Hollow-Fibre Gas Separator: The Effects of Process and Design Variables," *Ind. Eng. Chem. Process Des. Dev.*, **24**, 1015 (1985).
- Donahue, M. D., B. S. Minhas, and S. Y. Lee, "Permeation Behavior of Carbon Dioxide: Methane Mixtures in Cellulose Acetate Membranes," *J. Membr. Sci.*, **42**, 197 (1989).
- Lee, S. Y., B. S. Minhas, and M. D. Donahue, "Effect of Gas Composition and Pressure on Permeation through Cellulose Acetate Membranes," *New Materials and Processes for Separation, AIChE Symp. Ser.*, No. 261, **84**, 93 (1988).
- Pan, C. Y., "Gas Separation by Permeators with High Flux Asymmetric Membranes," *AIChE J.*, **29**, 545 (1983).
- Perrin, J. A., and S. A. Stern, "Separation of a Helium Methane Mixture in Permeators with Two Types of Polymer Membranes," *AIChE J.*, **32**, 1889 (1986).
- Rangarajan, R., M. A. Mazid, T. Matsuura, and S. Sourirajan, "Permeation of Pure Gases under Pressure through Asymmetric Porous Membranes: Membrane Characterization and Prediction of Performance," *Ind. Eng. Chem. Process Des. Dev.*, **23**, 79 (1984).
- Sidhoum, M., A. Sengupta, and K. K. Sirkar, "Asymmetric Cellulose Acetate Hollow Fibres: Studies in Gas Permeation," *AIChE J.*, **34**, 417 (1988).
- Stern, S. A., "Membrane Gas Separation," *Industrial Processing with Membranes*, Lacey and Loeb, eds., Wiley, New York (1972).

Manuscript received Apr. 24, 1990, and revision received Aug. 7, 1990.